CrystEngComm

PAPER

View Article Online
View Journal | View Issue

Cite this: *CrystEngComm*, 2024, **26**, 4073

Seed-assisted crystallization of high-silica cubic and hexagonal faujasite polymorphs in the presence of the tetraethylammonium (TEA^+) cation†

Corentin Chatelard,‡[ab] Raquel Martinez Franco,[b] Mathias Dodin[b] and Alain Tuel *[a]

Received 14th March 2024,
Accepted 29th April 2024

DOI: 10.1039/d4ce00257a

rsc.li/crystengcomm

Silica-rich Y (FAU topology) and EMC-2 (EMT topology) zeolites have been obtained in the presence of the tetraethylammonium (TEA^+) cation as a structure-directing molecule and the corresponding protonic zeolites as seeds. In the presence of USY seeds, Y zeolites were fully crystallized after a few hours at 130 °C but they were unstable and rapidly converted into chabazite, a zeolite with CHA topology. Their stability could nonetheless be greatly improved by decreasing the temperature to 110 °C without significantly modifying the morphology of the crystals and the composition of the framework. Framework SiO_2/Al_2O_3 ratios up to 13 could be obtained, which is the highest value ever reported for Y zeolites synthesized with TEA^+ cations as the sole organic molecule. The use of H-EMC-2 as seeds generally led to FAU–EMT intergrowths in which the relative proportion of EMT depended on the composition of the seeds. However, a pure EMT zeolite could be obtained under specific conditions. With a framework SiO_2/Al_2O_3 ratio of 11.2, it constitutes the first example of Si-rich EMT obtained in the absence of crown ether from conventional silica and alumina sources.

Introduction

The frameworks of zeolites Y (FAU topology) and EMC-2 (EMT topology) are both built up from sodalite cages *sod* and hexagonal prisms *d6r*.[1] Due to different linking of *sod* cages between the two zeolites, the symmetry of the FAU framework is cubic while that of EMT is hexagonal. Both zeolites can be synthesized with SiO_2/Al_2O_3 ratios up to 10 from gels with the same composition using crown ethers as structure-directing molecules.[2–5] However, crown ethers being relatively expensive, there is a significant demand for synthesis routes leading to similar framework compositions but using cheaper molecules. While micrometric crystals of the cubic structure (FAU) can be obtained with relatively high SiO_2/Al_2O_3 ratios in the presence or in the absence of organic molecules, this is not the case for the hexagonal structure (EMT), for which the use of 18-crown-6 remains necessary.[6] EMT zeolites with SiO_2/Al_2O_3 ratios up to 4.7 have been obtained by hydrothermal conversion of FAU zeolites in the presence of the 1,1′-(1,4-butanediyl)bis(1-azonia-4-azabicyclo[2,2,2]octane) ($[Dab\text{-}4]^+$) cation but zeolites were converted into AFX after 24 hours.[7] Attempts to crystallize EMT-type zeolites in the absence of seeds from organic-free systems always led to ultra-small nanocrystals with $SiO_2/Al_2O_3 < 3$, two disadvantages that limit their large-scale application in industry.[8,9] In the presence of more conventional organic molecules, all zeolites in which hexagonal domains were previously observed actually consisted of FAU–EMT intergrowths with a percentage of EMT ranging from *ca.* 15% in zeolite CSZ-1 to 85% in zeolite ECR-30.[10] Zeolites that contained the higher proportion of EMT were ZSM-20 and ECR-30, prepared in the presence of tetraethylammonium (TEA^+) and methyl-triethylammonium ($MTEA^+$) cations, respectively. The structure of ZSM-20, whose synthesis was first reported by Ciric in 1976, was definitely solved more than 20 years later by Newsam *et al.*[11,12] On the basis of transmission electron micrographs, the authors showed that ZSM-20 crystals contained intergrowths of extended blocks of pure cubic and hexagonal symmetries with approx. 70% EMT. A serious advantage of this zeolite compared to faujasite was that solids could be quite easily obtained with SiO_2/Al_2O_3 ratios up to 10.[13] ZSM-20 generally contains approx. 16 wt% organics, suggesting that TEA^+ cations serve as structure-directing cations for both the FAU

[a] *CNRS, IRCELYON, UMR 5256, Université Claude Bernard Lyon 1, 2 Avenue Albert Einstein, 69626 Villeurbanne Cedex, France.*
E-mail: alain.tuel@ircelyon.univ-lyon1.fr
[b] *IFP Energies Nouvelles, Rond-point de l'échangeur de Solaize, BP 3, 69360, Solaize, France*

† Electronic supplementary information (ESI) available. See DOI: https://doi.org/10.1039/d4ce00257a

‡ Present address: LGM, 1330 Avenue Guilibert de la Lauzière, 13100 Aix en Provence.

and EMT parts of the crystals. However, while pure FAU materials have been recently obtained in the presence of TEA^+ cations, this is not the case for the hexagonal polymorph.[14] One of the reasons is that ZSM-20 crystallizes under very specific conditions with TEAOH and that minor changes in the gel composition and/or heating conditions inevitably lead to the co-crystallization of other zeolites.[13]

Several recent papers have demonstrated the necessity to combine high temperatures along with seeds to crystallize FAU-type zeolites with high SiO_2/Al_2O_3 ratios in the presence of tetraalkylammonium cations.[15] Zhu and co-workers obtained Y zeolites with SiO_2/Al_2O_3 up to 15.6 from gels containing HY seeds and mixtures of tetrabutylammonium (TBA^+) and TEA^+ cations as organic structure directing agent (OSDA).[16] SiO_2/Al_2O_3 ratios to approx. 12 have been obtained within less than 4 h at 180 °C in the presence of tetrapropylammonium (TPA^+) cations.[17] Similar ratios to 15.9 were obtained in the presence of the TBA^+ organic cation after 3.5 days at 120 °C.[18] Even higher ratios (SiO_2/Al_2O_3 = 18.2) were observed very recently using the same TBA^+ cation after 16 h at 160 °C.[19] Although complete crystallization curves are rarely reported in the corresponding literature, it is suspected (or reported) that all of those faujasites are systematically obtained as intermediates in the crystallization of zeolites with higher densities, *i.e.* ZSM-5 with TPA^+ and ZSM-11 with TBA^+. The conversion is very fast at high temperature and the time span within which Y zeolites are pure and highly crystalline can be extremely narrow. Attempts to crystallize Y zeolites under similar conditions using TEA^+ instead of TBA^+ cations were unsuccessful and the solids obtained were either poorly crystallized or contaminated by zeolite beta for long crystallization periods.[19] To date, the highest SiO_2/Al_2O_3 ratios observed on Y zeolites obtained in the presence of TEA^+ cations as single OSDA do not exceed 9, which necessitates several days of crystallization at 120 °C in the presence of seeds.[16] We have previously reported the formation of [TEA^+]FAU zeolites as intermediates during the synthesis of chabazite (CHA) zeolites from gels containing TEAOH, conventional Si and Al sources and dealuminated faujasites (CBV 720) as seeds. [TEA^+]FAU was fully crystalized after 10 hours at 130 °C and characterized by SiO_2/Al_2O_3 = 8.5.[20] When a protonic EMC-2 was used as seeds instead of HY, the obtained zeolites were not purely hexagonal materials but mixtures of cubic and hexagonal phases, with possible formation of FAU–EMT intergrowths. XRD data revealed that the proportion of FAU in the intermediate zeolite depended on the aluminium content in the seeds, suggesting that a pure EMT polymorph could be obtained by carefully controlling the nature of seeds, the gel composition and crystallization conditions.

The present work reports a detailed study of the influence of the composition and structure of seeds on the nature of zeolites obtained using TEA^+ as structure directing cation. In particular, we show for the first time that under very specific conditions, the use of EMT seeds can lead to the crystallization of pure hexagonal materials with high silicon contents. Other parameters such as the synthesis time, the crystallization temperature and the overall SiO_2/Al_2O_3 of the gel are also considered.

Experimental

Synthesis of seeds

Seeds with the FAU topology were purchased from Zeolyst® with overall SiO_2/Al_2O_3 ratios from 5.2 (CBV 600) to 60 (CBV 760). Seeds with the EMT framework type were obtained from the dealumination of a [Na]EMC-2 zeolite synthesized following the method of Delprato *et al.*[2] Typically, 2.51 g of NaOH (Carlo Erba) and 7.93 g of $NaAlO_2$ (Riedel de Hahn, 54 wt% Al_2O_3, 41 wt% Na_2O) were dissolved in 34.8 mL H_2O, followed by the addition of 7.85 g of 18-crown-6 (Aldrich). After mixing for 10 min, 66.9 g of Ludox HS-30 (Aldrich) were slowly added under vigorous stirring and the obtained gel, with the following composition 10 SiO_2–Al_2O_3–2.2 Na_2O–0.87(18-crown-6)–140 H_2O was stirred at room temperature for 24 hours and heated under static conditions at 110 °C for 12 days. The highly crystalline zeolite with a framework SiO_2/Al_2O_3 ratio of 7.2 was calcined and exchanged with ammonium nitrate prior to dealumination. The NH_4^+-EMC-2 form of the zeolite was subjected to a series of steaming/acid washing for different periods at 600 °C and using 0.1 M HCl solutions. Various [H]EMC-2 zeolites were obtained with overall SiO_2/Al_2O_3 ratios, including both framework and extra-framework aluminium species, ranging from 7.2 to 64. The nature, structure and composition of all zeolite seeds used in this study are listed in Table 1.

Synthesis of zeolites

In a typical preparation, 5.308 g of TEAOH (Aldrich, 35 wt% in water) were mixed with 4.156 mL of water, followed by the addition of 0.357 g of NaOH and 0.2042 g of $NaAlO_2$. After stirring for a few minutes, the solution became completely clear and 4.765 g of colloidal silica (Ludox® AS-40) were added dropwise under vigorous stirring. After stirring the gel with the composition 27.6 SiO_2–0.76 Al_2O_3–11 TEAOH–4.8 Na_2O–511 H_2O for 20 hours, seeds were added (the Si content in the seeds corresponded to 10% of the total Si in the gel) and stirring was maintained for 2 additional hours. The gel was then placed in an autoclave and crystallized at temperatures between 70 and 130 °C under static conditions

Table 1 Main characteristics of the zeolites used as seeds

Zeolite	Form	SiO_2/Al_2O_3	S_{BET} ($m^2\ g^{-1}$)
CBV-100	Na^+	5.1	900[a]
CBV 400	H^+	5.1	730[a]
CBV 600	H^+	5.1	660[a]
CBV 712	NH_4^+	12	730[a]
CBV 720	H^+	32	780[a]
CBV 760	H^+	54	720[a]
CBV 780	H^+	83	780[a]
EMC-2	H^+	16	765[b]
EMC-2	H^+	18.2	786[b]
EMC-2	H^+	21.2	823[b]
EMC-2	H^+	25.4	851[b]
EMC-2	H^+	47.6	792[b]
EMC-2	H^+	64	815[b]

[a] Data from the supplier. [b] This work.

for different periods. After crystallization, autoclaves were cooled down in an ice bath and solids were recovered by filtration, washed with water and dried overnight at 80 °C. When necessary, part of the zeolite was calcined in air at 550 °C for 12 hours.

Characterization techniques

X-ray diffraction (XRD) patterns were recorded at room temperature on a Bruker D8 advance diffractometer (Cu Kα radiation) from 4 to 80° with 0.02° steps and 0.5 s per step. The crystallinity of the obtained zeolites was estimated by comparing the area of XRD reflections with that of the background between 5 and 30°.

The overall SiO_2/Al_2O_3 ratio of zeolites was measured by X-ray fluorescence (XRF) on a Panalytical Epsilon 4 analyser using a calibration curve previously established on a series of zeolites with well-known compositions. ICP measurements (HORIBA Jobin Yvon) were made on selected samples to check the accuracy of XRF data. In all cases, SiO_2/Al_2O_3 ratios were similar within ±5%.

The amounts of organics in the different zeolites were obtained by measuring the weight loss upon heating as-made solids in air in a Mettler Toledo Thermal Analysis apparatus. Samples were heated from 25 to 750 °C with a heating rate of 5 °C min^{-1}.

Scanning Electron Microscopy (SEM) images were obtained at 2 kV on a Zeiss Supra 40 microscope equipped with an Everhart–Thornley SE2 detector. After dispersion of the zeolite in ethanol, the solution was ultra-sonicated and deposited on an aluminium plot.

Transmission Electron Microscopy (TEM) images were obtained on a JEOL 2010 LaB6 microscope operating at 200 kV. Zeolites were embedded in an epoxy resin that was cut into slices of 60 nm using an ultramicrotome.

N_2 adsorption/desorption isotherms were measured at 77 K on a Belsorp-mini (BEL-Japan) sorption apparatus. *Circa* 50 mg of sample was outgassed under vacuum in a cell at 300 °C overnight prior to adsorption.

All nuclear magnetic resonance (NMR) spectra were recorded on a Bruker Avance III 500 WB spectrometer equipped with a double-bearing probe head. Samples were spun at 10 kHz in 4 mm zirconia rotors and data were collected at room temperature using a standard one-pulse sequence. Pulse lengths and recycle delays were 1 μs (π/6) and 1 s for ^{27}Al, and 2.5 μs (π/4) and 60s for ^{29}Si nuclei. Chemical shifts were referred with respect to the signal of $Al(H_2O)_6^{3+}$ species in a 1 M aqueous solution of $Al(NO_3)_3{\cdot}9H_2O$.

Results

Seeds with the FAU topology

We have previously reported that chabazite could be obtained after several days at 130 °C when CBV 720 (SiO_2/Al_2O_3 = 30) was used as seeds. Chabazite was not formed as a primary product but from the conversion of an intermediate [TEA^+]FAU zeolite, fully crystallized after *ca.* 10 hours. As for similar materials prepared with TPA^+ or TBA^+ cations, the fast crystallization could be attributed to a cooperative effect of seeds and high temperature.[17,18] At this temperature, the intermediate zeolite was almost systematically contaminated by CHA, suggesting that the FAU-to-CHA conversion started before or immediately after the complete crystallization of the faujasite.[19] The batch did not contain any trace of the hexagonal EMT polymorph and [TEA^+]FAU crystals appeared in the form of regular octahedra of *ca.* 1 μm, with a framework SiO_2/Al_2O_3 ratio of 8.5 ± 0.2, close to the highest value obtained in the literature with TEA^+ cations.[16] Beta zeolite, which is very often observed at this crystallization temperature was not formed either, probably because of the presence of FAU seeds and a high TEAOH content in the gel. The overall reaction pathway did not change at lower crystallization temperatures and [TEA^+]FAU zeolites were formed as intermediate solids even at temperatures as low as 70 °C. However, the time necessary to complete the crystallization of the [TEA^+]FAU zeolite increased from 10 hours at 130 °C to *ca.* 3 days at 70 °C. At the same time, decreasing the temperature considerably improved the stability of the intermediate [TEA^+]FAU, thus facilitating the recovery of the zeolite before the formation of CHA (Fig. 1). For comparison, a complete crystallization of [TPA^+]FAU took more than 4 days at 110 °C when TPA^+ cations were used as organic molecules under quite similar conditions.[17] [TEA^+]FAU zeolites obtained between 70 and 130 °C possess very similar SiO_2/Al_2O_3 ratios as measured by XRF, indicating that crystallization temperature has a minor effect on the framework composition (Table S1, ESI†).

In order to minimize the quantity of seeds in the crystallization process, additional syntheses were performed at 3 different temperatures (90, 110 and 130 °C) while decreasing the amount of CBV 720 from 10 to 2.5 wt% in the precursor gel. Regardless of the crystallization temperature, the amount of seeds did not significantly modify the

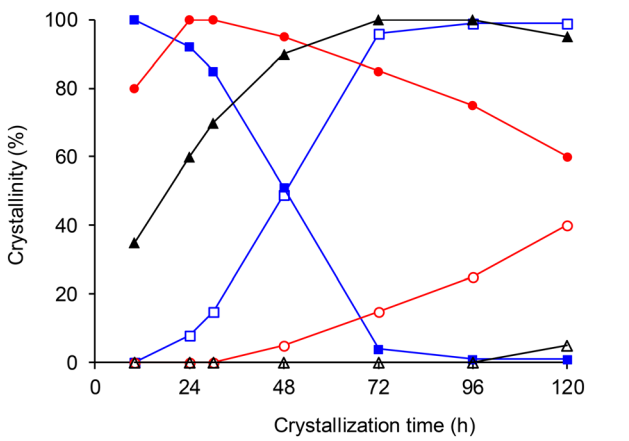

Fig. 1 Evolution of the percentages of as-made FAU (full symbols) and CHA (open symbols) zeolites with the crystallization period at 130 °C (squares), 110 °C (circles) and 70 °C (triangles) of gels containing 10 wt% CBV 720 as seeds.

crystallization kinetics of the [TEA$^+$]FAU zeolite. As an example, syntheses performed at 130 °C with 10 and 2.5 wt% seeds gave fully crystallized [TEA$^+$]FAU zeolites after 10 hours. However, the quantity of seeds had a strong influence on the composition of the zeolite (Table S2, ESI†). For all three temperatures, the SiO_2/Al_2O_3 ratio of the zeolite increased with the amount of CBV 720 added to the synthesis gel and the maximum was always obtained with 10 wt% seeds. The alkalinity of the precursor gel had only a minor influence on the composition of the zeolite while changing significantly the kinetics of crystallization. At 110 °C, the time needed to obtain a fully crystalline faujasite increased from 1 to 3 days when the Na_2O/SiO_2 ratio of the gel was decreased from 0.17 to 0.14. At the same time, the framework SiO_2/Al_2O_3 ratio of the [TEA$^+$]FAU zeolite increased by only 12% and attempts to further reduce the NaOH content or the amount of TEAOH in the gel led to lower crystallinities, with the presence of amorphous phase in the XRD patterns (Table S3, ESI†).

On the other hand, the composition was significantly affected by the nature of the zeolite seeds. As shown in Fig. 2, syntheses performed with various commercial FAU-type zeolites showed that the SiO_2/Al_2O_3 ratio of the [TEA$^+$]FAU framework increased linearly with the SiO_2/Al_2O_3 of the seeds, from 7.6 with CBV 600 (SiO_2/Al_2O_3 = 5.2) to 9.0 for CBV 760 (SiO_2/Al_2O_3 = 60). Since all syntheses were performed with 10 wt% seeds at 110 °C for 1 day, those differences were attributed to the change in the gel composition upon addition of seeds. Indeed, the overall SiO_2/Al_2O_3 of the precursor gel increased from *ca.* 30 with CBV 600 to 40 with CBV 760. Experiments performed with zeolite CBV 100 that possesses the same SiO_2/Al_2O_3 as CBV 600 were unsuccessful, likely because of the high Na content and the low solubility of the zeolite in alkaline solutions.

In a similar way, the use of the high-silica CBV 780 (SiO_2/Al_2O_3 = 80) gave essentially amorphous materials, indicating that FAU-type zeolites could crystallize only from seeds in the H^+ or NH_4^+ forms and within a limited range of compositions. Data are in line with those previously reported in the literature for Y zeolites prepared with tetraalkylammonium cations as structure directing molecules. The use of seeds with various compositions not only affected the crystallization kinetics, but it also modified the final composition with an increase of the SiO_2/Al_2O_3 ratio of the zeolite with that of the seeds.[18,19]

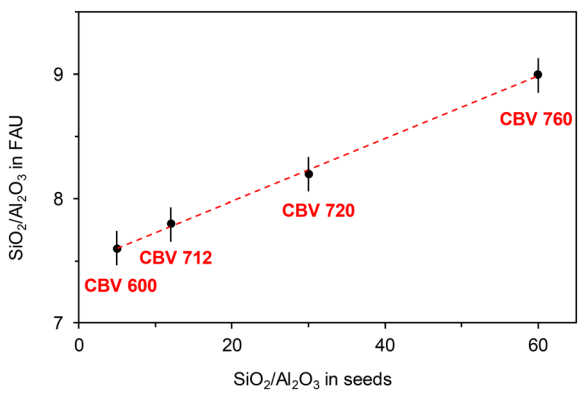

Fig. 2 Composition of the intermediate FAU zeolite with the SiO_2/Al_2O_3 ratio of seeds. Vertical bars correspond to an error of ±0.15 on the measurements of the composition by XRF.

Data obtained using different HY zeolites as seeds have suggested that the SiO_2/Al_2O_3 ratio of the [TEA$^+$]FAU zeolite increases with the Si content in the synthesis gel. A series of gels with various SiO_2/Al_2O_3 ratios between 25 and 200 was prepared by changing the amount of $NaAlO_2$. The amount of seeds (10 wt% CBV 720) and crystallization conditions (1 day at 110 °C) were unchanged. For each synthesis, the amount of NaOH was adjusted in order to keep the Na_2O/SiO_2 ratio constant and avoid a change in pH value. In all cases a highly crystalline FAU zeolite was obtained, indicating that the change in the composition of the gel did not significantly affect the kinetics of crystallization. In contrast to the pH value, decreasing the aluminium content in the gel had a substantial influence on the composition of the final zeolite. Indeed, the SiO_2/Al_2O_3 ratio of the [TEA$^+$]FAU zeolite increased with the SiO_2/Al_2O_3 ratio of the gel from *ca.* 7.2 for SiO_2/Al_2O_3 = 25 to *ca.* 13 for SiO_2/Al_2O_3 = 200 (Table 2).

At the same time, the solid yield decreased from 48% at low SiO_2/Al_2O_3 to *ca.* 35% for the zeolite with SiO_2/Al_2O_3 = 13. The evolution of the zeolite composition with that of the precursor gel clearly showed that the SiO_2/Al_2O_3 ratio of the solid tended to a limit and could not exceed 14 under the present synthesis conditions (Fig. 3). Attempts to go beyond this limit by using a more siliceous zeolite such as CBV 760 as seeds or higher SiO_2/Al_2O_3 ratios in the gel were not successful.

Nonetheless, this limit represents the highest value ever reported for Y zeolites obtained after 1 day at 110 °C and following a direct synthesis route in the presence of the sole TEA$^+$ cation.

TGA/DSC curves of sample 4 (Table 2) showed two main losses between 25 and 800 °C (Fig. S1, ESI†). The first one between 25 and 200 °C is associated to an endothermic peak and corresponds to the removal of water. The second one of about 10 wt% between 300 and 700 °C is attributed to the exothermic decomposition of organic molecules. It corresponds to 9.3 TEA$^+$ cation per unit cell, that is, approx.

Table 2 SiO_2/Al_2O_3 ratios of intermediate FAU zeolites with the SiO_2/Al_2O_3 ratio of the gel prior to seeds addition

	SiO_2/Al_2O_3	
Sample	Gel	Solid
1	25	7.2
2	36	7.8
3	50	9.0
4	60	9.6
5	70	11
6	80	11.2
7	100	11.4
8	150	12.7
9	200	13

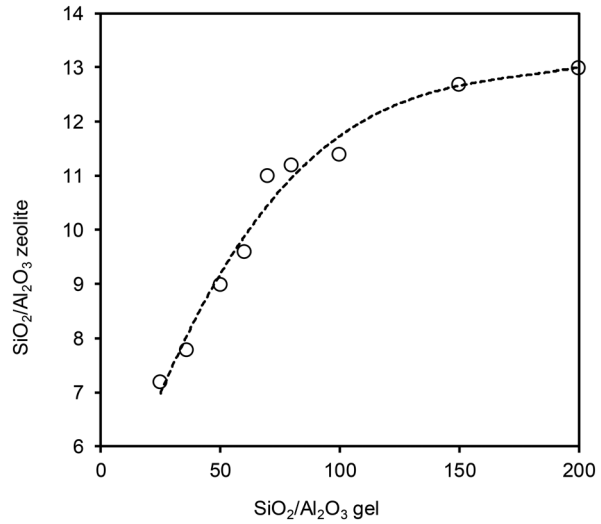

Fig. 3 Evolution of the composition of the intermediate FAU zeolite with the overall silica-to-alumina ratio in the synthesis gel.

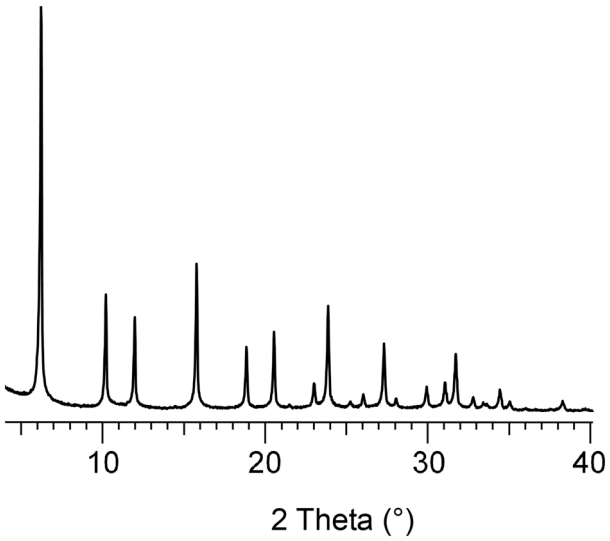

Fig. 4 PXRD pattern of the calcined FAU zeolite with SiO_2/Al_2O_3 = 13 (sample 9, Table 2).

1.15 TEA^+ per supercage. The Na_2O/Al_2O_3 ratios obtained by XRF on the different samples were systematically below 1. For sample 4 (Table 2), the value Na_2O/Al_2O_3 = 0.67 corresponds to *ca.* 3.2 Na^+ per supercage (SiO_2/Al_2O_3 = 9.6 corresponds to 4.3 Al atoms per supercage). Combining results from TGA and XRF gives 1.15 TEA^+ + 3.2 Na^+ = 4.35 cations per supercage, which corresponds exactly to the number of Al atoms. Compared to a NaY zeolite prepared in the absence of organics, these results suggest that some of the TEA^+ cations substitute for Na^+ to balance the negative charge of the framework. Moreover, the number of TEA^+ per supercage was in the range 1.15–1.4 for all samples and did not significantly change with the SiO_2/Al_2O_3 ratio of the zeolite. Liu *et al.* found quite similar values of *ca.* 1.1 TEA^+ per supercage in [TEA^+]FAU with SiO_2/Al_2O_3 = 7.76 and 1.3 TBA^+ in [TBA^+]FAU with SiO_2/Al_2O_3 = 15.9.[13,18] After heating at 550 °C for several hours, the solid was white and the intensity of the corresponding XRD pattern showed that the zeolite was stable at high temperature (Fig. 4).

The ^{29}Si NMR spectrum of the calcined zeolite with SiO_2/Al_2O_3 = 13 consists of 3 main signals between −110 and −90 ppm (Fig. 5a). In standard Y zeolites, these peaks are assigned to **Si**$(OSi)_4$, **Si**$(OSi)_3(OAl)$ and **Si**$(OSi)_2(OAl)_2$ sites, respectively, and their respective intensities are used to calculate the framework SiO_2/Al_2O_3 ratio.[20] Attempts to decompose the signal with 3 symmetrical lines did not give acceptable results and the corresponding SiO_2/Al_2O_3 ratio was always lower than 11.5. Decomposition was greatly improved by adding a fourth line to take the asymmetry of the signal around −100 ppm into account (Fig. S2, ESI†).

The additional line appeared at −98.2 ppm and corresponded to *ca.* 8% of the total intensity of the signal (Table S4, ESI†). Considering the value of the chemical shift, this line could be assigned to O_3SiOH species in the zeolite framework.[18,21] As it will be discussed below, those silanol groups likely result from defects created during the partial desilication of zeolite seeds. Assuming that only the peak at −100.5 ppm corresponds to **Si**$(OSi)_3(OAl)$ species, the framework SiO_2/Al_2O_3 ratio was estimated at 13.4, in excellent agreement with the value obtained by XRF (Table S3, ESI†). The small difference between the values obtained by XRF and by decomposition of the ^{29}Si NMR signal could be explained by a minor dealumination of the zeolite upon calcination, as evidenced by the presence of a small signal at −2 ppm in the ^{27}Al NMR spectrum (Fig. 5b).

Such a signal, which corresponds to octahedrally coordinated extra-framework Al species, is generally not observed on NaY zeolites synthesized in the absence of organic molecules. However, it is always present in the corresponding HY zeolites because AlO_4 tetrahedra are less stable in the framework when the negative charge is compensated by protons.[21] In the case of [TEA^+]FAU zeolites, protons are generated upon calcination of organic cations at high temperature, which results in a partial dealumination of the zeolite.

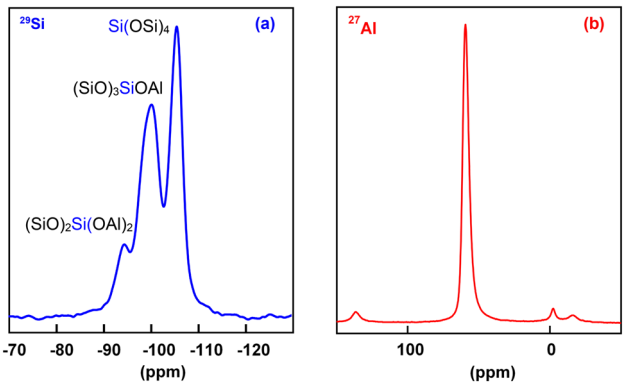

Fig. 5 ^{29}Si (a) and ^{27}Al (b) MAS NMR spectra of the calcined FAU with SiO_2/Al_2O_3 = 13.

The N_2 adsorption–desorption isotherm of the zeolite obtained with SiO_2/Al_2O_3 = 100 in the gel (sample 7 in Table 2) shows characteristics of types I and IV isotherms, typical of solids with micro and mesopores (Fig. S3, ESI†). The BET surface area and micropore volume are 700 $m^2\ g^{-1}$ and 0.26 $cm^3\ g^{-1}$, respectively, in agreement with values usually reported in the literature for Y zeolites synthesized in the presence of tetraalkylammonium cations.[13,18] The presence of a hysteresis loop with abrupt closure at $p/p_0 \approx 0.45$ in the desorption branch indicates the presence of mesopores that are mainly located inside the crystals and communicate with the surface *via* entrances smaller than 4 nm.[22,23]

The morphology of the zeolite consists of aggregated octahedra with individual sizes between 0.5 and 1 μm, quite similar to those of CBV 720 crystals (Fig. 6). However, the surface is smooth and differs from that of CBV 720 crystals by the absence of mesopores, thus supporting partial recrystallization of the seeds. Ultramicrotome sections of a calcined zeolite with SiO_2/Al_2O_3 = 11.4 reveal that individual crystals are not homogeneous but possess a core–shell structure formed by a purely microporous shell surrounding a highly mesoporous core, suggesting that the zeolite crystallizes from species in solution around partially desilicated CBV 720 seeds (Fig. S4, ESI†). This structure explains the presence of the hysteresis loop in N_2 adsorption–desorption isotherms as well as the existence of silanol defects in the ^{29}Si NMR spectrum of the zeolite. However, despite a heterogeneous structure, the composition of the crystals is quite homogeneous, with SiO_2/Al_2O_3 ratios in the internal core and in the external shell very similar to the value determined by XRF (Fig. S4, ESI†).

Seeds with the EMT topology

Although seeds appear to be essential to get pure Si-rich FAU zeolites, the role they really play during crystallization is still a matter of debate. Actually, seeds are supposed to partially dissolve in the alkaline medium and serve as support for a surface-induced nucleation in the presence of organic molecules. With the tetraethylammonium (TEA^+) cation, only FAU-type zeolites are formed in the presence of HY seeds; solids with the EMT topology are never observed, though their frameworks are built up by linking the same SBUs, but in a different manner. The situation is totally different when seeds added to the synthesis mixture possess the EMT topology instead of the FAU topology. Preliminary experiments had shown that products recovered after 1 day were not pure hexagonal polymorphs but FAU–EMT mixtures or intergrowth structures, with a proportion of FAU that depended on the composition of the seeds.[20]

A series of syntheses was first performed using the initial gel composition 27.6 SiO_2 – 0.76 Al_2O_3 – 11 TEAOH – 4.8 Na_2O – 511 H_2O, and adding [H]EMC-2 seeds with various SiO_2/Al_2O_3 ratios, typically from 7.2 to 64. XRD patterns of calcined zeolites confirmed the presence of the FAU topology in most of the solids, characterized by an intense (111) reflection at 2θ = 6.2° (Fig. 7).

In all cases the amount of zeolite formed largely exceeded that of the seeds introduced in the synthesis gel, with yields >90% based on the Al content. The proportion of FAU seemed to be more important for HEMT seeds with high (64) and low (7.2) SiO_2/Al_2O_3 ratios. For intermediate compositions, XRD patterns are similar to those already reported in the literature for FAU–EMT intergrowth structures. The quantification of FAU and EMT proportions is difficult on the basis of powder XRD, particularly when one of the fractions is lower than 20%, because most of the reflections characteristic of the cubic polymorph are also present in EMC-2. Moreover, some of the reflections characteristic of the hexagonal structure can be significantly broadened by faults in the crystals, resulting from the intergrown structure of the solids. Nonetheless, the proportions of FAU and EMT polymorphs in all zeolites can be roughly estimated by visually comparing experimental XRD patterns with those obtained using the DIFFaX program developed by J. M. M. Treacy, simulating randomly stacking faujasite layers in infinitely thick crystals.[10] Patterns were first simulated over the whole 2θ range (Fig. 7) and then optimized between 5 and 13°, a region in which signals are very sensitive to the composition (Fig. S5, ESI†). Proportions obtained for the best fit between experimental and simulated spectra are listed in Table S5 (ESI†). Only seeds with SiO_2/Al_2O_3 ratios between 20 and 30 give zeolites with a high proportion of EMT, with a maximum for SiO_2/Al_2O_3 = 25.4, all others giving materials with more than 40% FAU. As for FAU seeds, the overall SiO_2/Al_2O_3 ratio of the final zeolite increases with that of EMT seeds (Table S5, ESI,† entries 1, 5, 6 and 9–12).

A series of additional syntheses showed that the nature of the zeolite depends not only on seed composition but also on crystallization parameters and gel composition. In particular, the percentage of EMT in zeolites obtained using Si-rich seeds (SiO_2/Al_2O_3 = 64) slightly increased with the amount of aluminium introduced the synthesis gel, but the best results never exceeded 60% for SiO_2/Al_2O_3 = 15 (Table S5, ESI,† entries 1–4). Decreasing the SiO_2/Al_2O_3 ratio in the gel below 12 led to the formation of zeolite beta in addition to FAU–EMT intergrowths. In a similar way, the

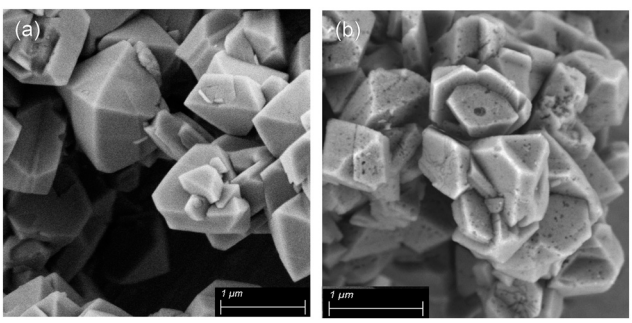

Fig. 6 SEM image of the FAU zeolite with SiO_2/Al_2O_3 = 13 (a) and CBV 720 (b).

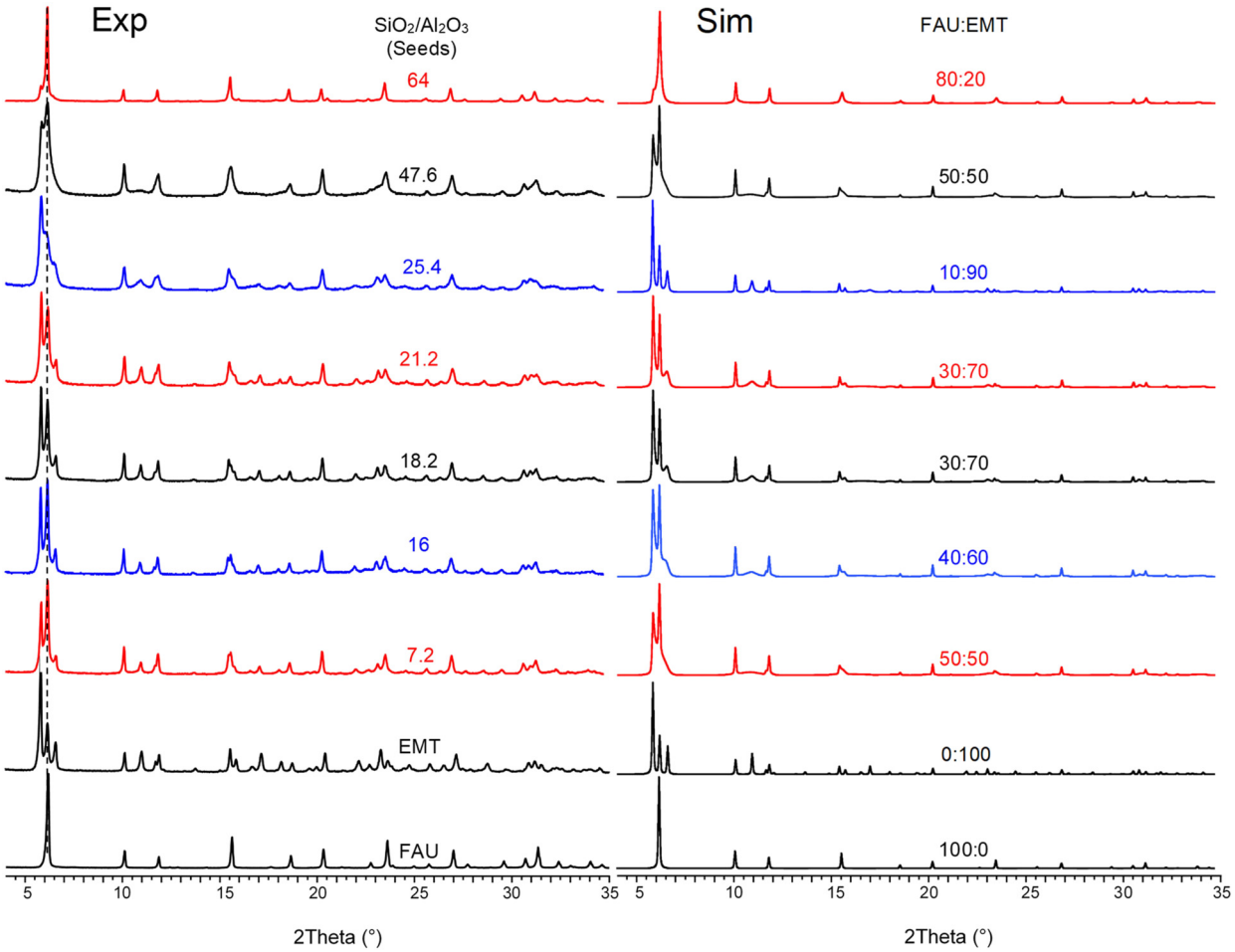

Fig. 7 XRD patterns of calcined zeolites obtained in the presence of HEMT seeds with various SiO_2/Al_2O_3 ratios. Left: experimental patterns; right: simulated patterns using the DIFFaX program developed by J. M. M. Treacy[10] with the relative percentages of FAU and EMT. Patterns of pure FAU and EMT and their simulations are also displayed. The dashed line corresponds to the position of the (111) reflection of the FAU structure.

crystallization of EMT was not significantly favoured by decreasing the Al content of the gel when seeds with SiO_2/Al_2O_3 = 7.2 were used (Table S5, ESI,† entries 12–14). Only a combination of seeds with intermediate compositions (SiO_2/Al_2O_3 = 25.4) and gels with low Al contents ($50 < SiO_2/Al_2O_3 < 80$) yielded zeolites with XRD patterns very similar to those of EMT materials obtained in the presence of crown-ethers (Fig. 8).

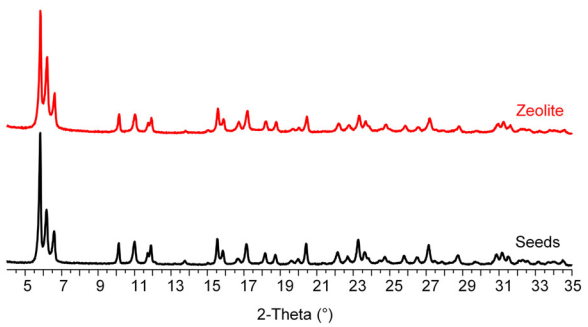

Fig. 8 XRD patterns of HEMT (SiO_2/Al_2O_3 = 25.4) used as seeds (bottom) and the corresponding calcined zeolite obtained from a gel with SiO_2/Al_2O_3 = 80 (top).

The presence of FAU domains in these solids cannot be totally excluded but their density in the framework is such that they cannot be detected by standard XRD. Within this range of composition, solid yields were >95% with respect to the overall Al content in the gel (between 40 and 50% with respect to Si), indicating that zeolites did not simply result from the desilication of seeds but also from the crystallization of Si and Al precursors. For SiO_2/Al_2O_3 = 80 in the gel, crystallization was confirmed by comparing the XRD pattern of the final zeolite with that of the solid recovered immediately before the hydrothermal treatment (Fig. S6, ESI†). Prior to crystallization, most of the solid phase was amorphous and only weak reflections corresponding to EMT seeds could be observed. After 1 day at 110 °C, the solid was highly crystalline with a framework SiO_2/Al_2O_3 of 11.2, and all the amorphous material had disappeared. Crystallization was also supported by the presence of organic molecules in the porosity of the zeolite.

A weight loss of *ca.* 17 wt% was observed between 300 and 650 °C upon heating the as-made zeolite in air, which corresponds to 9.8 TEA^+ cations per unit cell (not shown). This value is very close to that previously observed in ZSM-20, a FAU–EMT intergrowth structure containing predominantly hexagonal EMT crystallites.[24] Additional evidence for crystallization of Si and Al species came from the major difference between the size of seeds (1.5 μm) and that of zeolite crystals, which appeared in the form of small hexagonal crystals of *ca.* 0.1 μm (Fig. 9).

Discussion

Intergrowth can occur between two distinct, but related zeolite structures when the sequence of stacking of layers along one axis of the crystal is modified. This modification can be the result of recurrent twinning in the original structure, as it is the case for some of the members of the FAU–EMT family. Despite similar structural features, the formation of the intergrowth can generate local stress at the interface between the two structures, due to essentially minor differences in unit cell dimensions, composition and/or in energy of the corresponding frameworks. Although NaY crystals are commonly considered as having a purely cubic defect-free structure, HRTEM revealed that they may actually contain a significant density of faults, even when the zeolite has been synthesized in the absence of organic molecules.[25] Those faults mainly consist of twinning on (111) planes, involving reflection across a mirror plane intersecting the supercages and passing through the *d6r* units. In contrast to materials such as ZSM-20 or ECR-35, twinning planes in FAU frameworks are generally isolated from each other and separate two cubic domains, without any evidence for the presence of extended regions of hexagonal structure. In the absence of hexagonal domains, zeolite layers growing on the surface of FAU seeds will preferentially adopt the cubic symmetry, especially as it was reported that, for the same composition, the hexagonal framework is slightly higher in energy than the cubic one.[26]

This may explain why EMT structures have never been observed when syntheses are performed with USY seeds. On the contrary, previous publications have reported that the framework of EMC-2, prepared using 18-crown-6 molecules, is never purely hexagonal but always contains a significant proportion of FAU domains, as revealed by high-resolution TEM.[27] Though dealumination of Y zeolites in acidic media has been widely documented in the literature, data concerning the hexagonal EMC-2 are scarce. Nonetheless, it has been reported that HY and HEMC-2 zeolites react similarly to steaming/acid-washing dealumination cycles without significant differences in framework stability.[28] Under such conditions, the proportion of FAU and EMT in the seeds is supposed to be the same, regardless of the extent of dealumination. However, experiments clearly indicate that the structure of the final zeolite strongly depends on the Al content in the seeds. One explanation could be that the change in the overall composition of the gel upon addition of seeds is such that it favours the formation of one of the zeolites but previous experiments performed using seeds with SiO_2/Al_2O_3 = 25.4 showed the absence of FAU over a broad range of gel compositions. Moreover, this would not explain why the proportion of FAU in the final zeolite first decreases and then moves back up with the SiO_2/Al_2O_3 ratio of the seeds. A second explanation for this phenomenon could result from the extent of desilication of the seeds during the aging period at room temperature. Desilication can be roughly estimated by recording the XRD pattern of the solid phase recovered at room temperature just before the hydrothermal treatment (Fig. S7, ESI†). Seeds with low SiO_2/Al_2O_3 give XRD patterns that contain peaks characteristic of the EMT topology along with amorphous phase. For intermediate ratios, XRD reflections of the EMT topology are still visible but they are broader and their intensity is weak, suggesting that the structure of the seeds has been significantly damaged. With highly dealuminated seeds, the corresponding XRD patterns are shapeless and characterize totally amorphous materials. This follows trends that have been previously reported for the desilication of Y zeolites with various aluminium contents, that is, Al-rich zeolites are quite resistant to desilication while Si-rich zeolites are not.[29] Highly dealuminated USY zeolites can even entirely collapse in alkaline media, as it is the case for EMT seeds with $SiO_2/Al_2O_3 > 50$. Poorly desilicated seeds probably still contain FAU domains in the crystals, that act as USY seeds and favour the co-crystallization of the cubic polymorph in the presence of TEA^+ cations. Many studies have reported that desilication of twinned zeolite crystals in alkaline media preferentially occurred at defective areas of the framework, in particular intergrowth boundaries.[30,31] Under such conditions, moderate desilication observed for seeds with SiO_2/Al_2O_3 = 25.4 may suppress most of the FAU domains, leaving seeds with almost defect-free, purely hexagonal structures. Concerning the most siliceous seeds, their efficiency is probably considerably reduced after their complete amorphization, and crystallization gives solids similar to those obtained in the absence of seeds.

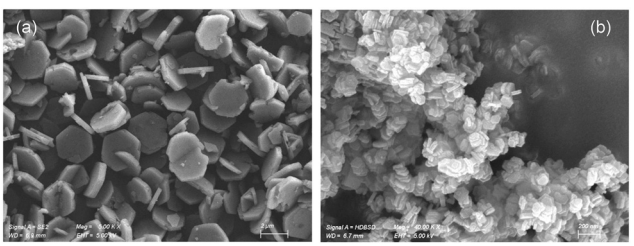

Fig. 9 TEM images of HEMT zeolite (SiO_2/Al_2O_3 = 25.4) used as seeds (a) and the corresponding zeolite (b) obtained with SiO_2/Al_2O_3 = 80 in the gel prior to addition of seeds.

Conclusion

Zeolites have been synthesized at low temperature from alkaline gels containing the tetraethylammonium cation as

structure directing molecule and seeds with the FAU and EMT topologies. Despite similar structures built up from *sod* cages and *d6r* units, the kind of seeds strongly influenced the crystallization and the nature of the zeolites formed. The use of USY seeds (FAU topology) with various SiO_2/Al_2O_3 ratios always led to pure Y zeolites, obtained as intermediates in the crystallization of CHA. Their composition depended not only on the SiO_2/Al_2O_3 ratio of the seeds but also on the Al content in the gel. With CBV 720 as seeds, framework SiO_2/Al_2O_3 ratios up to 13 could be obtained, which constitutes the highest value for Y zeolites synthesized from conventional Si and Al sources in the presence of TEA^+ cations. With EMT seeds, the synthesis was less selective and the obtained zeolites were almost systematically FAU–EMT intergrowths. The low selectivity was attributed to the presence of FAU domains in EMC-2 crystals, acting as USY seeds and directing the crystallization of the cubic polymorph. Nonetheless, pure hexagonal materials could be obtained by carefully controlling the composition of seeds and the Al content in the gel. EMC-2 zeolites with SiO_2/Al_2O_3 ratio up to 11.2 could be obtained using 10 wt% seeds with SiO_2/Al_2O_3 = 25.4, which constitutes the first example of Si-rich EMT obtained in the absence of crown ether from conventional silica and alumina sources.

Author contributions

C. C.: methodology, data collection, investigation; R. M. F.: conceptualization, funding acquisition, project administration, supervision, writing – review; M. D.: conceptualization, funding acquisition, project administration, supervision, writing – review; A. T.: methodology, data collection, supervision, writing – original draft, writing – review and editing.

Conflicts of interest

There are no conflicts to declare.

Acknowledgements

This work was financially supported by IFPEN within the framework of a PhD grant (C. C.).

References

1 Database of zeolite structures, Available online, **http://www.iza-structure.org/databases/**.
2 F. Delprato, L. Delmotte, J. L. Guth and L. Huve, *Zeolites*, 1990, **10**, 546–552.
3 C.-N. Wu and K.-S. Chao, *J. Chem. Soc., Faraday Trans.*, 1995, **91**(1), 167–173.
4 E. J. P. Feijen, K. De Vadder, M. H. Bosschaerts, J. L. Lievens, J. A. Martens, P. J. Grobet and P. A. Jacobs, *J. Am. Chem. Soc.*, 1994, **116**, 2950–2957.
5 S. L. Burkett and M. E. Davis, *Microporous Mater.*, 1993, **1**, 265–282.
6 W. Lutz, *Adv. Mater. Sci. Eng.*, 2014, **2014**, 724248.
7 K. Matsuda, N. Funase, K. Tsuchiya, N. Tsunoji, M. Sadakane and T. Sano, *Microporous Mesoporous Mater.*, 2019, **274**, 299–303.
8 Y. Wang, J. Zhang, X. Meng, S. Han, Q. Zhu, N. Sheng, L. Wang and F.-S. Xiao, *Microporous Mesoporous Mater.*, 2019, **286**, 105–109.
9 E.-P. Ng, J.-M. Goupil, A. Vicente, C. Fernandez, R. Retoux, V. Valtchev and S. Mintova, *Chem. Mater.*, 2012, **24**, 4758–4765.
10 M. M. J. Treacy, D. E. W. Vaughan, K. G. Strohmaier and J. M. Newsam, *Proc. R. Soc. A*, 1996, **452**, 813–840.
11 J. Ciric, *US Pat.*, 3972983, 1976.
12 J. M. Newsam, M. M. J. Treacy, D. E. W. Vaughan, K. G. Strohmaier and W. J. Mortier, *J. Chem. Soc., Chem. Commun.*, 1989, 493–495.
13 D. He, D. Yuan, Z. Song, Y. Tong, Y. Wu, S. Xu, Y. Xu and Z. Liu, *Chem. Commun.*, 2016, **52**, 12765–12768.
14 N. Dewaele, L. Maistriau, J. B. Nagy, Z. Gabelica and E. G. Derouane, *Appl. Catal.*, 1988, **37**, 273–290.
15 J. Li, M. Gao, W. Yan and J. Yu, *Chem. Sci.*, 2023, **14**, 1935–1959.
16 D. Zhu, L. Wang, D. Fan, N. Yan, S. Huang, S. Xu, P. Guo, M. Yang, J. Zhang, P. Tian and Z. Liu, *Adv. Mater.*, 2020, **32**, 2000272.
17 Y. Sada, S. Miyagi, K. Iyoki, M. Yoshioka, T. Ishikawa, Y. Naraki, T. Sano, T. Okubo and T. Wakihara, *Microporous Mesoporous Mater.*, 2022, **344**, 112196.
18 D. Zhu, L. Wang, W. Cui, J. Tan, P. Tian and Z. Liu, *Inorg. Chem. Front.*, 2022, **9**, 2213–2220.
19 D. Zhu, L. Wang, W. Zhang, D. Fan, J. Li, W. Cui, S. Huang, S. Xu, P. Tian and Z. Liu, *Angew. Chem., Int. Ed.*, 2022, **61**, e202117698.
20 C. Chatelard, M. Dodin, R. Martinez-Franco and A. Tuel, *Microporous Mesoporous Mater.*, 2022, **340**, 112028.
21 J. Klinowski, *Prog. Nucl. Magn. Reson. Spectrosc.*, 1984, **16**, 237–309.
22 J. C. Groen and J. Pérez-Ramirez, *Appl. Catal., A*, 2004, **268**, 121–125.
23 J. C. Groen, L. A. A. Peffer and J. Pérez-Ramirez, *Microporous Mesoporous Mater.*, 2003, **60**, 1–17.
24 S. Ernst, G. T. Kokotailo and J. Weitkamp, *Zeolites*, 1987, **7**, 180–182.
25 M. Audier, J. M. Thomas, J. Klinowski, D. A. Jefferson and L. A. Bursill, *J. Phys. Chem.*, 1982, **86**, 581–584.
26 I. Petrovic, A. Navrotsky, M. E. Davis and S. I. Zones, *Chem. Mater.*, 1993, **5**, 1805–1813.
27 J. L. Lievens, J. P. Verduijn, A.-J. Bons and W. J. Mortier, *Zeolites*, 1992, **12**, 698–705.
28 O. Cairon, *ChemPhysChem*, 2013, **14**, 244–251.
29 D. Verboekend, G. Vile and J. Perez-Ramirez, *Adv. Funct. Mater.*, 2012, **22**, 916–928.
30 C. S. Cundy, M. S. Henty and R. J. Plaisted, *Zeolites*, 1995, **15**, 342–352.
31 T. Li, J. Ihli, Z.-Q. Ma, F. Krumeich and J. A. van Bokhoven, *J. Phys. Chem. C*, 2019, **123**, 8793–8801.